

A Broadband Electron Spectrometer and Electron Detectors for Laser Accelerator Experiments

C. E. Clayton, K. A. Marsh, C. Joshi, C. B. Darrow^{a)},
A. E. Dangor^{b)}, A. Modena^{b)}, Z. Najmudin^{b)}, and V. Malka^{c)}

Department of Electrical Engineering
University of California at Los Angeles
56-125B Engineering IV
Los Angeles, CA 90024

Abstract

We describe the apparatus used to measure the spectrum of accelerated electrons from a laser-plasma acceleration experiment carried out at Rutherford Appleton Laboratories (RAL). The source of the broadband, energetic electrons was the forward Raman scattering instability of a high intensity ($5 \times 10^{18} \text{ W/cm}^2$) laser. Here the laser beam photons decay into scattered photons and a relativistic electron plasma wave. The plasma wave subsequently accelerates plasma electrons to relativistic energies.[1] The spectrometer and detectors were designed to give a quantitative (in energy and flux) single-shot electron spectrum over as wide a range of energies as possible. In this paper we present some calibration measurements taken prior to the RAL run which agree very well with TRACE3D runs used to model the beam transport. The silicon surface barrier detector (SBD) arrangement and fluorescer-film-pack arrangement are also described. Finally, some preliminary results are obtained which show excellent agreement between the spectra obtained with the SBD's and the film.

INTRODUCTION

The laser is the short pulse VULCAN laser[2] at Rutherford Appleton Laboratories operating at around 25 TW in a sub-ps pulse. The plasma is produced when the laser ionizes a pulsed jet of hydrogen gas exiting a high Mach number nozzle. The typical electron densities of the resultant plasma are in the range of $1 \times 10^{19} \text{ cm}^{-3}$ for a jet backing pressure of 20 bar.

ELECTRON SPECTROMETER

The electron spectrometer is shown in Fig. 1(a). It consists of a pair of pole pieces energized by a "C" electromagnet, and a vacuum box. The vacuum box is bolted to the vacuum chamber in the RAL target bay. The exit of the lead aperture is 54 cm from the gas jet and laser focus giving a collection angle of $f/60$ or 1° full angle. The tilted exit plane of the vacuum box is made so that the different energies are in focus along the length of the exit plane. The detectors are shown placed several cm away from the exit in order to take advantage of the fact that the electrons move in a straight line whereas x-ray noise within the chamber will fall off rapidly as the detectors are moved back. Note that the electron

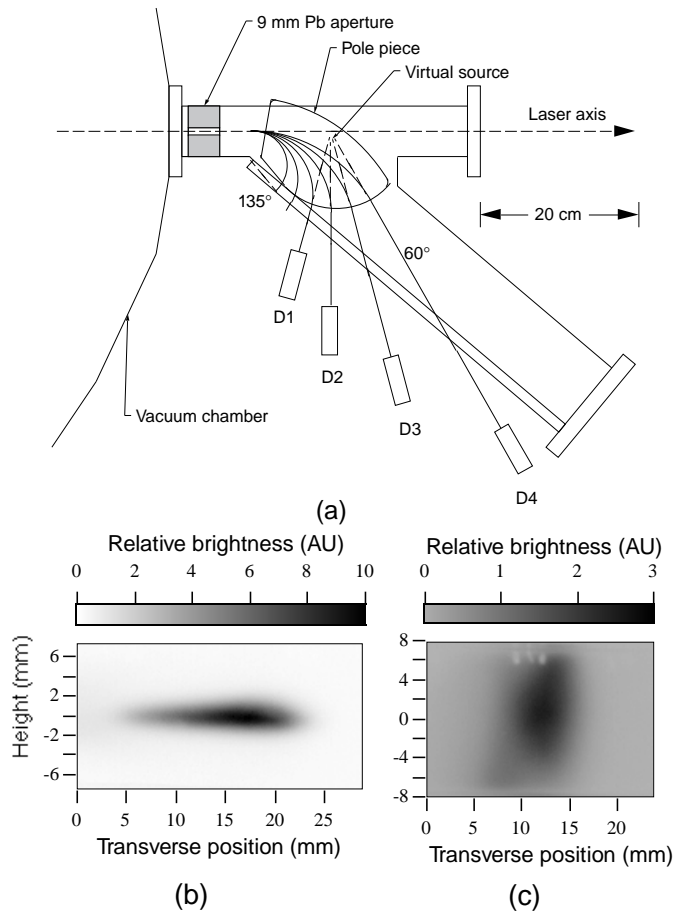


Figure 1: (a) Schematic of electron spectrometer and 4 channel SBD detector array. The pole piece is a Browne & Buechner type[4] with a 10° pole-face rotation at the entrance to provide some vertical focusing. Electron trajectories are shown for bending angles of 135° – 60° in 15° steps. (b) focal plane image of stigmatic focal point for "switcher" type pole shape. (c) Focal plane image of the Browne & Buechner design as shown in (a). Vertical focusing is much weaker with the B&B shape although energy coverage is greater.

trajectories projected back into the vacuum box tend to intersect at a single point under the pole piece. This is called the "virtual source" for the electron spectrum.

Prior to taking the spectrometer to RAL, it was bench-tested with a 2 MeV electron linac at UCLA.[3] Figs. 1(b) and (c) show the results of this test for two different pole pieces. Figure 1(b) shows a nice, stigmatic focus obtained

This work is supported by DOE contract number DE-FG03-92ER40727.

using “switcher” pole pieces[4] (semi-circular shaped). The beam enters on flat side which is rotated by 8° to provide additional vertical focusing. The physical location of this stigmatic focus, i.e., focusing in energy as well as vertically, is within a few mm of the location predicted by TRACE3D runs. Figure 1(b) therefore is the spectrum of the 2 MeV electron beam showing a $\approx 5\%$ droop in the tail. The shape of the same beam using the Browne and Buechner pole pieces, as was used in the RAL experiment, is shown in Fig. 1(c). In this case, the pole pieces are focusing in the energy direction but not in the vertical direction, even with the 10° pole-face rotation. Rather, the beam is approximately collimated vertically at all energies. The location of the energy focal plane lies along the exit to the vacuum box.

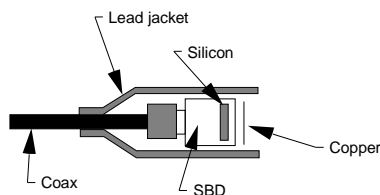


Figure 2: Cross-sectional view of the shielded surface barrier detectors used for quantitative electron flux measurements. The lead jacket (≈ 3 mm thick) shields the surface barrier detector from background x-rays in the room while the $200\ \mu\text{m}$ thick copper pieces (3 for a total of $600\ \mu\text{m}$) will transmit energetic electrons but block the soft x-rays exiting the vacuum chamber. With this configuration, the electron signal to x-ray signal was better than 10:1.

THE DETECTOR SETUP

The layout of 4 SBD's is shown in Fig. 1(a). Figure 2 shows a cross-section of one of these detectors. The lead and copper shields are used to reduce the x-ray background to a manageable level. The coaxial cable length was about 10 m which was necessary to move the preamplifiers away from the electrically-noisy environment close to the vacuum chamber. The preamps were EG&G Model 113 “scintillator”, charge-sensitive preamps which had a variable integrating capacitor in parallel to the cable capacitance.

Because the expected electron spectrum is exponential in energy, we wanted to configure the detectors so that the sensitivity would be much lower for detector D1 than for detector D4 thereby increasing the single-shot dynamic range of the measurement. The variable capacitor was one of the ways used to vary the sensitivity of individual detectors by switching in extra capacitance. Also, different silicon thickness' were used, with detectors D1 and D2 being $500\ \mu\text{m}$ thick and detectors D3 and D4 being $1\ \text{mm}$ thick. Also, each detector has a relationship between bias voltage and “depletion thickness” or active thickness. This, too, can be used to vary an individual detectors' sensitivity by varying the active thickness of the $500\ \mu\text{m}$ detectors to, say, $200\ \mu\text{m}$ by dropping the bias voltage down from it's maximum or fully-depleted value. When a detector is not fully biased, the waveform seen on an oscilloscope will have two distinct

components—a fast-rising part due to charge deposited within the depletion region and a slower-rising part due to charge deposited in the field-free region which nevertheless drifts into the detection circuit. Thus by recording the fast-rise portion of the waveform, one is recording the portion only from the thinner depletion region. (This technique was verified at UCLA using the 2 MeV linac to expose the detectors at some middle-scale value. The fast part of the signal was observed to increase linearly with depletion depth. Also measured was the effective parallel capacitance which was found to be about $300\ \text{pF}$ for the EG&G 113 preamps attached to 10 m of 50 ohm coaxial cable.) Apertures are not useful as beam attenuators for non-collimated beams at these energies since the range of a 13 MeV electron (the typical value at D1) is nearly an inch in lead.

THE FILM / FLUORESCER SETUP

As an alternative to the electronic detectors discussed earlier, we attempted to acquire a spectrum on film which was sandwiched between two sheets of 3M “Trimax” fluorescer. The fluorescers were cut to the width of the 35 mm film (Ilford HP5 Plus, ISO 400) and the entire 36 cm long sandwich was slid into a black plastic ($0.5\ \text{mm}$ thick) cassette and the end was sealed against room light with black tape. The cassette was placed either in contact with the exit flange of the vacuum box, i.e., in the energy plane of the spectrometer (near field), or placed 5 cm away from the vacuum box but still parallel to the flange (far field). The film was developed for 5 minutes in D19 developer.

The film data can be obtained on the same shot as the data on the detectors. This is because the areal density of the film + fluorescers + plastic cassette is negligible for the energies measured on the film ($13.6\text{--}32.6\ \text{MeV}$) being about $1/30$ of a stopping range for the lowest energy.

The developed film was converted to “density” using a 12 bit CCD and a calibrated density step-wedge taped up to a lightbox. The estimated density-accuracy of this measurement is ± 0.05 . The density was converted to relative exposure using an experimentally-measured replica of a density step wedge taken on the same ISO 400 film and developed in the same way as the data thereby indicating the nonlinear “gamma” of the film. Thus the 2-D image of the film taken with the CCD was converted into $\text{Log}(\text{Exposure})$ vs. position on the film. Finally, the horizontal position on the film was converted to electron energy by the known relationship between radius of curvature of the electron (proportional to momentum) and position on the film.

EXPERIMENTAL RESULTS

In this section we present examples of data from both types of detectors—film and SBD's—taken on the very same shot. But first we will look at two images taken with the film which demonstrate that the electrons do indeed appear to come from a “virtual source” under the pole pieces.

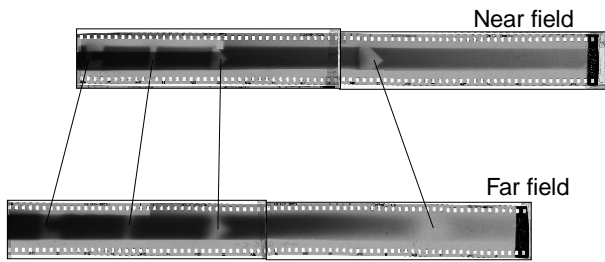


Figure 3: Two images of accelerated electrons taken on two similar laser shots with the film / fluorecser cassette located in two different planes: Near field, against the exit flange of the spectrometer; and Far field, 5 cm away from—and parallel to—the exit flange. Four lead objects were placed against the vacuum window, about 1 cm in front of the near field position. The measurement shows the directional nature of the electrons and the fact that they appear to emanate from a “virtual source”.

Film images

Figure 3 shows the near-field and far-field images taken on two similar shots showing single-shot spectra from 13.6–32.6 MeV in the near-field case. Four pieces of lead of various shapes and about 6 mm thick were placed at the exit window (76 μm Mylar) of the vacuum box, about 1 cm in front of the film in the near-field case. For the far-field case, the lead was not moved yet the “shadows” of the electrons have moved in such a way as to indicate that the electrons appear to emanate from a virtual source under the pole piece, just as sketched in Fig. 1(a).

An Electron spectrum

An electron spectrum was taken on both diagnostics on the same shot by putting the film cassette in the near-field position and viewing the SBD signals on the oscilloscopes as usual. Although there will be an energy-dependent scattering angle from the film, the estimated smearing of a beamlet at the low energies is on the order of the beam size so that the net drop in flux seen on the 8 mm diam SBD is small.

Rather than plot the raw signal vs. energy from the SBD’s, we have transformed the data into electrons/MeV vs. MeV. Thus the area under the graph is the absolute number of electrons. The conversion to measured volts/detector on the oscilloscope to electrons/detector was made by using the known energy dissipation rate dE/dx into ionization of the silicon detector, the known thickness dx of the detector, the resultant free charge produced (electrons/dE), and finally the

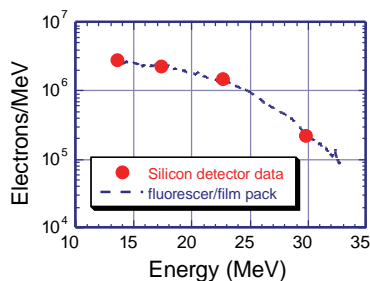


Figure 4: Electron spectra obtained by the SBD detectors (points) and by the film / fluorecser combination (curve) for the same shot in hydrogen gas. The film data was scaled vertically only to overlap the SBD data.

known charge-sensitivity of the preamplifiers (V/coulomb). Now, since each detector is about 8 mm wide in the energy direction (0.8 cm/detector), we can use the known dispersion (cm/MeV) to finally put our measured volts/detector into electrons/MeV at the MeV location of the detector. There is one final correction factor needed and that is that the detector is vertically smaller than the beam and this roughly factor-of-two is included to estimate the total flux of electrons, not just those that hit the detector. This is what is plotted in the four points in Fig. 4. A similar routine was performed on a 10 pixel wide lineout down the center of the spectrum taken simultaneously on film. Now one can consider the horizontal pixel discreteness in the same way as discrete detectors and use the transformation: $\text{signal/pixel} \times \text{pixels/cm} \times \text{cm/MeV} = \text{signal/MeV}$. Finally, the same vertical correction, based on TRACE3D runs, is applied across the energy axis. The only free parameter for comparing this spectrum to the SBD spectrum is the unknown sensitivity, i.e. fluorescence photons per electron. Thus we are free to scale the film data vertically in Fig. 4 and have done so. We see that the two spectra agree very well over an order of magnitude in electrons/MeV.

One might question why the agreement. The answer is that both are ionization-based detectors. The amount of light given off by the Trimax fluorecser is proportional to the amount of energy deposited through ionization giving a linear relationship between exposure on the film and electron flux which is completely analogous to the quantity of free charge induced on the SBD’s vs. electron flux.

ACKNOWLEDGMENTS

The authors are grateful to Dr. D. Neely, C. Danson and the rest of the Vulcan Laser staff at RAL for their expert assistance throughout this experiment.

^{a)} Lawrence Livermore National Laboratory, Livermore, USA.

^{b)} Imperial College, London, U.K.

^{c)} Ecole Polytechnique, Palaiseau, FR.

REFERENCES

1. A. E. Dangor, A. Modena, Z. Najmudin, C. E. Clayton, K. A. Marsh, C. Joshi, C. B. Darrow, V. Malka, C.N. Danson, “Wavebreaking of Relativistic Plasma Waves”, submitted to Nature.
2. C. N. Danson, L. J. Barzanti, Z. Chang, A. E. Demerell, C. B. Edwards, S. Hancock, M. H. R. Hutchinson, M. H. Key, S. Luan, R. R. Mahadeo, I. P. Mercer, P. Norreys, D. A. Pepler, D. A. Rodkiss, I. N. Ross, M. A. Smith, P. Taday, W. T. Toner, K. W. M. Wigmore, T. B. Winstone, R. W. W. Wyatt, and F. Zhou, “High contrast multi-terawatt pulse generation using chirped pulse amplification on the VULCAN laser facility”, Opt. Comm. 103, 392-397 (1993).
3. C. E. Clayton and K. A. Marsh, “A 2 MeV, 100 mA electron accelerator for a small laboratory environment”, Rev. Sci. Instr. 64, 728-731 (1993).
4. H. A. Enge, “Deflecting magnets”, in *Focusing of Charged Particles*, edited by A. Septier (Academic, Ney York, 1977) ch. 4.2; J. J. Livingood, *The Optics of Dipole Magnets* (Academic, Ney York, 1969).